Revue RAMReS – Sciences Appliquées et de l'Ingénieur
RAMReS 2025 - *Published Online 2026* - http://publication.lecames.org/
Vol. 7(1), pp. 64-74, Online January 2026

Vol. 7
ISSN 2630-1164
December 2025

Full Length Research Paper

Engineering of Structural, Magnetic and Electronic Properties of Planar Aluminene through Transition Metal Doping: An ab initio Study

Pape Sene[1,2*], Allé Dioum[1,2], Sossé Ndiaye[2], El Hadji Oumar Gueye[2], Jean Paul Latyr Faye[2], Omar Faye[2,3], Kharouna Talla[2]

[1]Material–Composite Systems and Applications (MASCA), Physics Department, Cheikh Anta Diop University (UCAD), Dakar, Senegal
[2]Solid State Physics and Materials Science Group, Physics Department, Cheikh Anta Diop University of Dakar, 5005 Dakar, Senegal
[3]Solid State Physics and Materials Science Group, Physics Department, Cheikh Anta Diop University of Dakar, 5005 Dakar, Senegal

Received June 2025 – Accepted October 2025

**Corresponding author. .....paaco125@gmail.com.....*

Abstract:

Aluminene, a two-dimensional material composed solely of aluminum atoms, has recently attracted considerable attention due to its remarkable stability and intriguing electronic features. In this work, we focus on the effects of doping planar aluminene with 3d and 4d transition metals, using first-principles calculations based on density functional theory (DFT) as implemented in Quantum ESPRESSO with Projector Augmented Wave (PAW)PAW, , Optimized Norm-Conserving Vanderbilt (ONCV)ONCV and Ultrasoft USPP pseudopotentials. Pseudopotentials (USPP).

The results reveal that transition metal doping significantly modifies the structural, electronic, and magnetic properties of aluminene. Structural analysis indicates that while certain dopants preserve the near-hexagonal geometry, others induce strong distortions that alter the lattice parameters and bond angles. From the electronic perspective, all doped systems maintain their metallic nature, although the band structures and densities of states (DOS and PDOS) show pronounced dopant-dependent features.

A particularly notable effect is the emergence of magnetism with specific transition metal dopants, such as V, Cr, Mn, Fe, Mo, and Nd, which generate substantial magnetic moments, reaching up to 5.38 μB/cellμ_B⁄cell in the case of manganese. Conversely, dopants such as Sc, Ti, Cu, and Zn maintain a non-magnetic state. The binding energies further highlight the diverse chemical stability of the different configurations, reflecting the strength of interaction between the dopant and the aluminene host lattice.

These findings provide valuable insights into the tunability of aluminene through transition metal doping and open perspectives for its exploitation in spintronic devices.

Keyword : Planar aluminene, transition metals, DFT, stability, magnetic properties, electronic properties, spintronics.

Cite this article:
Pape Sene, Allé Dioum, Sossé Ndiaye, El Hadji Oumar Gueye, Jean Paul Latyr Faye, Omar Faye, Kharouna Talla. (2025). Engineering of Structural, Magnetic and Electronic Properties of Planar Aluminene through Transition Metal Doping: An ab initio Study. Revue RAMReS – Sci. Appl. & de l'Ing., Vol. 7(1), pp. 64-74. ISSN 2630-1164.

1. Introduction

Two-dimensional (2D) materials have revolutionized materials science over the past two decades due to their unique physical properties and promising technological applications [1–4]. Since the discovery of graphene in 2004 [1], intensive research has focused on other 2D systems such as silicene [2], phosphorene [3], and transition metal dichalcogenides (TMDs) [4]. These atomically thin materials exhibit high electron mobility, mechanical flexibility, and a large specific

surface area, paving the way for diverse applications in electronics, optoelectronics, catalysis, energy storage, and spintronics [17, 19, 21, 22].

To fully exploit their potential, it is essential to be able to precisely tune and control their intrinsic properties. Doping, which involves the controlled introduction of foreign atoms or defects, has emerged as a key strategy to modulate their band structure, conductivity, magnetic response, and chemical reactivity [17–19, 21–23, 25]. Doping methods include substitutional doping, charge transfer doping, and atomic vacancy doping, each modulated for specific applications [17, 19, 21, 23].

Among these approaches, doping with transition metals (TMs) is particularly promising. Due to their partially filled d orbitals, these atoms can introduce new magnetic and electronic functionalities into materials that are initially non-magnetic [17, 19, 21–23]. In graphene and TMDs, the incorporation of transition metals like Mn, Cr, or Fe has enabled the induction of magnetic moments, modification of the density of states at the Fermi level, and the generation of complex hybridization effects [17, 21, 22]. This approach opens up prospects for applications in spintronics and magnetoresistance [13].

Literature Review of Aluminene

Aluminene, an atomically thin sheet composed exclusively of aluminum, has recently been proposed as a new stable 2D system [5, 6]. Theoretical studies have confirmed its mechanical and dynamic stability, as well as its intrinsic metallic nature [5–7]. Aluminene, although composed of a single element, possesses a delocalized electronic structure that offers potential for engineering its properties via external modifications, particularly doping with transition metals. This approach is part of a general perspective demonstrated for numerous 2D materials, where doping with transition metals allows for the effective modulation of electronic and magnetic properties, thus paving the way for applications in spintronics [8].

The existing literature highlights the great versatility of aluminene as a platform for property engineering. First-principles studies have explored the effects of various dopants, such as transition metals, alkali metals, alkaline-earth metals, and light elements like boron, carbon, and nitrogen [25-30].

- **Transition Metal Doping:** The adsorption of TMs can induce localized electronic states and enhance gas adsorption, particularly for hydrogen storage via the Kubas mechanism [28, 30]. This doping can also impart magnetic properties, which are essential for spintronics and gas sensors [28].

- **Alkali and Alkaline-Earth Metal Doping:** The adsorption of Li, Na, or K on aluminene influences its structural and mechanical properties significantly. While the metallic character of aluminene remains preserved upon decoration (Pandey et al. 2019) [27]. Furthermore, Ca, Mg, or K can improve the material's rigidity and elastic modulus [29].

- **Light Element Doping:** The adsorption of light atoms like N, C, or B creates strong chemical bonds and transfers charge from aluminene to the dopant. Nitrogen doping, in particular, is studied for its ability to stabilize hydrogen, making it interesting for energy storage applications [26, 30].

Motivation and Objectives

Despite these studies, the field of engineering aluminene's magnetic properties through substitutional transition metal doping remains largely unexplored. Understanding how dopants perturb the hexagonal symmetry and electronic structure of the lattice is essential for predicting the feasibility of experimental synthesis. The metallic nature of pristine aluminene, primarily derived from the aluminum p-orbitals [7], is expected to be altered by the incorporation of transition metal atoms. These atoms introduce localized d-states near the Fermi level, modifying the density of states (DOS) and potentially inducing new electronic and magnetic properties, as observed in other two-dimensional doped materials like graphene and $MoSi_2N_4$ [9-11]. While pure aluminene is non-magnetic [5, 6], the introduction of transition metals can generate magnetic moments, a phenomenon well-documented in doped graphene [9, 14].

In this work, we systematically study the structural, electronic, and magnetic properties of planar aluminene doped with 3*d* and 4*d* transition metals. Using first-principles calculations within the framework of density functional theory (DFT) with the Quantum ESPRESSO package [15, 16], we analyze the impact of dopants on lattice parameters, binding energies, electronic band structures, densities of states, and magnetic moments. Our results reveal that some dopants preserve the non-magnetic character of aluminene, while others, such as V, Cr, Mn, Fe, Mo, and Nd, induce a significant magnetization, reaching up to 5.38 μ_B per cell.

2. Computational Method

The calculations were performed within the framework of density functional theory (DFT) using the Quantum ESPRESSO simulation package [15, 16]. Exchange–correlation effects were described by the generalized gradient approximation (GGA) in the PBEsol formulation [31]. Electron–ion interactions were modeled using projector augmented-wave

(PAW), ultrasoft pseudopotentials (USPP), and optimized norm-conserving Vanderbilt pseudopotentials (**ONCV**) [32-34].

A 3×3 supercell of planar aluminene, containing 18 atoms, was considered, with one Al atom substituted by a transition-metal dopant (representing a concentration of ≈5.5%). To suppress spurious interactions between periodic images, a vacuum spacing of 17.83 Å was introduced along the out-of-plane direction.

The choice of pseudopotentials and cutoff energies was guided by the Standard Solid-State Pseudopotential (**SSSP**) Efficiency library for PBEsol (version 1.3) [35]. We systematically employed values equal to or higher than the recommended cutoffs from this library, as provided by the Materials Cloud QE Input Generator [36]. The specific pseudopotentials used include, for example, Al.pbesol-n-kjpaw_psl.1.0.0.UPF [37], and y_pbesol_v1.4.uspp.F.UPF from the GBRV library [38]. This approach ensures a consistent balance between computational efficiency and accuracy for all dopants.

The plane-wave kinetic energy cutoff (E_{cut}) was set between 40 Ry and 90 Ry depending on the dopant and pseudopotential type, with corresponding charge density cutoffs (Ecutρ). Brillouin zone integrations were performed using Monkhorst–Pack meshes of at least 10×10×1, while denser grids (up to 25×25×1) were adopted for density of states (DOS) and band structure calculations. The diagonalization scheme used was the Davidson algorithm.

All structural optimizations were carried out until the convergence thresholds for total energy (etot_conv_thr=1.8×10−4 Ry) and force (forc_conv_thr=1.0×10−4 Ry/Bohr) were reached. Spin-polarized calculations were systematically included to capture any possible magnetic ordering.

The binding energy per atom ($E_B/atom$) was calculated by taking the difference between the total energy of the doped aluminene supercell (E_{tot}) and the sum of the reference energies of the isolated constituent atoms, weighted by their quantities. The result is then normalized by the total number of atoms (N) in the system. Mathematically, this is expressed as:

$$E_B/atom = \frac{E_{tot} - \sum n_i E_i}{N} \quad \text{[Eq 1]}$$

This methodology is widely used to evaluate the cohesive stability of 2D materials. It has been specifically applied to aluminene in previous studies, such as those by Kamal and Ezawa (2015) [5] and Yuan et al. (2017) [6].

Tableau 1.:. Computational parameters used

Dopant type	E_{cut} (Ry)	$E_{cutrhô}$ (Ry)	Notes
Most 3d & 4d TMs	40–60	240–480	Stable convergence
Mn	65	780	Higher cutoff required
Fe	90	1080	Strongly localized 3d
Co, Ni	45	360	Convergence issues

3. Results and Discussion

3.1. Structural Stability and Lattice Parameters

The planar structure of pristine aluminene was first optimized to establish a reference for the doped systems. Consistent with the work of Sene et al. [7], our calculations yielded optimized primitive cell lattice parameters of a=b=4.458 Å.

For our study, we used a 3x3 supercell, which was generated from the primitive cell using the Phonopy code [39]. The structural optimization of this supercell was then performed with Quantum ESPRESSO (DFT calculations). The optimized lattice parameters for this supercell are a=b=13.3325 Å, c=17.8328 Å, α=β=90° and γ=120°. These results confirm that the system retains its initial hexagonal symmetry. Figure 1 illustrates this planar structure and its different views.

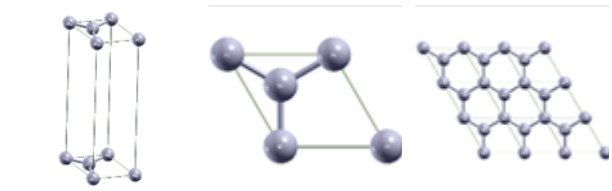

(a) 3D Structure (b) 2D Structure (c) Top view of 2D 3 units cell

Figure 1 : **Structure of the planar aluminene**

3.1.1. Doping with 3d Transition Metals

Figure 2 illustrates the evolution of the lattice parameters (a,b) and the γ angle after the substitutional doping of aluminene with elements from the 3*d* series. In most cases (Sc, Ti, V, Cr, Mn, Fe, Cu, Zn), the hexagonal structure is largely preserved, with very small variations around γ=120°. The fluctuations in the lattice parameters a and b are limited (≈ ±0.0001 Å), which demonstrates the structural robustness of the lattice against this type of doping.

However, two particular cases are worth noting:

- The $CoAl_{17}$ supercell did not converge after several optimization attempts. Investigations are currently underway to resolve this issue, including testing different diagonalization algorithms and refining the convergence parameters.

- The $NiAl_{17}$ supercell optimization is still in progress, so the results for this dopant are not included in this study.

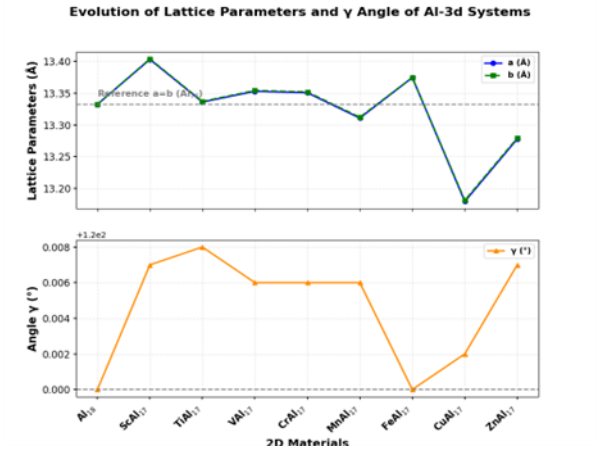

Figure 2 : **Al-3d lattice parameters and γ angle**

3.1.2. Doping with 4d Transition Metals

Figure 3 illustrates the evolution of the structural parameters after the insertion of 4*d* transition metals. For most systems (Y, Zr, Nb, Mo, Tc, Ru, Ag, Cd), the hexagonal symmetry is preserved, with a=b and γ≈120°. These results confirm good compatibility between aluminene and these dopants.

However, two particular cases stand out:

$RhAl_{17}$ and $PdAl_{17}$ show a break in hexagonal symmetry, with a≠b and γ≠120∘. This behavior indicates a significant distortion of the lattice, likely due to the atomic size and strong interactions between the *d* orbitals of these elements and the *p* orbitals of aluminum. These distortions can strongly influence the associated stability and electronic properties.

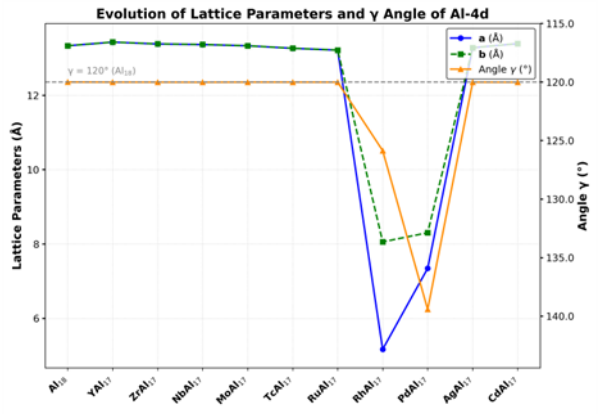

Figure 3 : **Al-4d lattice parameters and γ angle.**

Overall, these results demonstrate that aluminene exhibits remarkable structural stability when doped with 3*d* and 4*d* elements, with a few notable exceptions involving late transition metals (Rh, Pd). This paves the way for a more in-depth analysis of their electronic and magnetic properties.

Consistency with Literature

Our results on the structural stability of planar aluminene are in agreement with existing literature. We confirm that pristine aluminene maintains its γ≈120∘ angle, as predicted by Kamal et al. [5] and confirmed by Yuan et al. [6].

Doping with most 3*d* and 4*d* transition metals preserves the hexagonal lattice symmetry, demonstrating its robustness. However, the observed symmetry breaking (a ≠ b, γ ≠ 120∘) for Rh and Pd dopants is a well-known phenomenon in the engineering of 2D materials (Du et al., 2021 [40]). This behavior is explained by the strong hybridization between the *d* orbitals of these late transition metals and the *p* orbitals of aluminum. The review by Du et al. [40] as well as other studies of Zhang et al., 2022 and Zhang et al., 2018 [41,42] confirm that doping is a powerful lever for controlling symmetry and the resulting emergent properties, such as magnetism, in two-dimensional materials.

3.2. Binding Energies and Thermodynamic Stability

To evaluate the relative stability of the systems, we calculated the binding energy per atom ($E_B/atom$) as defined in Section 2. For the pristine aluminene 3x3x1 supercell, we obtained a value of -0.1894 Ry/atom, which is consistent with previous literature results [5, 6]. Table 2 and 3 summarize the $E_B/atom$ of TMs doping aluminene.

3.2.1. Doping with 3d Transition Metals

The calculated binding energies for the 3*d*-doped systems range from -0.1757 to -0.1915 Ry/atom (see Table 2). The stability follows this order (from least to most stable): Mn<Fe<Zn<V<Cr<Sc<Ti<Cu. This indicates that the $CuAl_{17}$ system is the most stable with an energy of -0.1915 Ry, while $MnAl_{17}$ is the least stable at -0.1757 Ry. These variations reflect the diverse interactions between the *d* orbitals of the dopants and the *p* orbitals of aluminum.

3.2.2. Doping with 4d Transition Metals

The binding energies for the 4*d* dopants vary between -0.1789 and -0.2855 Ry/atom. The order of increasing stability is: Mo < Zr < Cd < Nd < Tc < Ru < Y < Ag < Pd < Rh (see Table 3). This reveals two distinct trends. While dopants like Mo and Zr lead to relatively less stable configurations, Rh and Pd show significantly lower energies (-0.2855 and -0.2763 Ry, respectively). This suggests a strong energetic stabilization despite the hexagonal symmetry breaking observed in Section 3.1. These results indicate that structural stability and energetic stability do not always align, particularly for late transition metals.

3.3. Magnetic Properties

The introduction of transition metal dopants into the inherently non-magnetic pristine aluminene lattice induces a variety of magnetic behaviors.

3.3.1. Doping with 3d Transition Metals

While pristine aluminene is intrinsically non-magnetic, several dopants from the 3*d* series, namely V, Cr, Mn, and Fe, induce significant magnetic moments. The calculated absolute magnetizations range from 4.38 to a high of 5.38 $\mu_B/cell$ for $MnAl_{17}$.This demonstrates the ability of 3*d* transition metals to introduce strongly polarized, localized states in two-dimensional materials, a key step for spintronic applications. In contrast, other dopants in this series (Sc, Ti, Cu, and Zn) maintain the host material's non-magnetic state.

3.3.2. Doping with 4d Transition Metals

Among the 4*d* series, only Zr, Mo, Tc, and Ru develop a magnetic response, with absolute magnetizations between 1.38 and 4.57 $\mu_B/cell$The most notable case is $MoAl_{17}$, which reaches 4.57 $\mu_B/cell$. Whereas, dopants such as Y, Rh, Pd, Ag, and Cd show no magnetization, suggesting that the magnetic tendency of 4*d* dopants is more restricted than that of the 3*d* series. This tunability highlights the potential of doped aluminene as a versatile platform for engineering magnetic properties.

Tableau 2.: Properties of 3d-Doped Aluminene

Dopant (3d)	$E_B/atom$ (Ry/atom)	Total Magnetization (μ_B/cell)	Absolute Magnetization (μ_B/cell)
Sc	-0.1893	0.00	0.00
Ti	-0.1904	0.00	0.00
V	-0.1873	4.34	5.03
Cr	-0.1844	4.80	5.31
Mn	-0.1756	-3.65	5.38
Fe	-0.1793	2.43	4.38
Cu	-0.1915	0.00	0.00
Zn	-0.1807	0.00	0.00

Tableau 3: Properties of 4d-Doped Aluminene

Dopant (4d)	$E_B/atom$ (Ry/atom)	Total Magnetization ($\mu_B/cell$)	Absolute Magnetization ($\mu_B/cell$)
Y	-0.1872	0.00	0.00
Zr	-0.1799	1.71	2.78
Nb	-0.1819	3.31	4.49
Mo	-0.1788	3.65	4.57
Tc	-0.1809	2.05	3.32
Ru	-0.1860	1.12	1.38
Rh	-0.2855	0.00	0.00
Pd	-0.2763	0.00	0.00
Ag	-0.1896	0.00	0.00
Cd	-0.1818	0.00	0.00

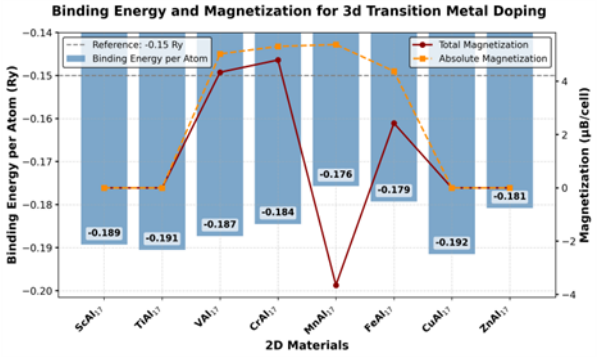

Figure 4 : $E_B/atom$ **& magnetization Al-3d**

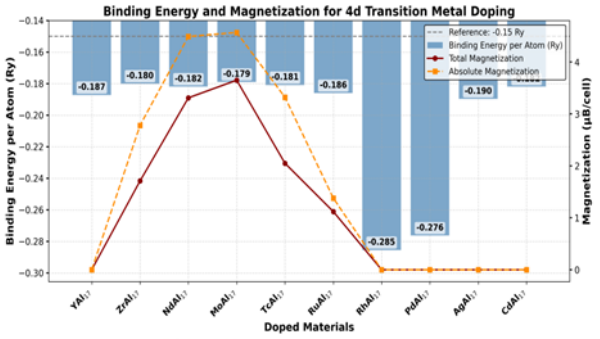

Figure 5 : $E_B/atom$ **& magnetization Al-4d**

Conclusion of Stability and Magnetic Properties

The investigation into the stability and magnetic properties of aluminene demonstrates its remarkable tunability via transition metal doping. While the majority of dopants preserve the material's hexagonal structure, late 4*d* elements like Rh and Pd induce significant structural distortions, highlighting a trade-off between structural and energetic stability.

More importantly, the study reveals that aluminene's non-magnetic nature can be engineered for spintronic applications. A significant number of 3*d* and 4*d* dopants successfully introduce large magnetic moments, with notable values for Cr, V, Fe, and Mo. A particularly interesting finding is that among all the dopants, only manganese (Mn) induces a negative total magnetization, a unique behavior that warrants further investigation. This suggests that the type of dopant can be finely tuned to not only introduce magnetism but also control its specific characteristics.

Notably, a correlation was observed between the magnetic state and the binding energy: non-magnetic systems tend to exhibit more negative binding energies, indicating they are more thermodynamically stable than their magnetic counterparts. This factor is crucial for potential applications, as it suggests a trade-off between magnetic functionality and structural stability. This makes doped aluminene a highly promising platform for next-generation magnetic devices.

3.4. Electronic Properties: Band Structure and Density of States (DOS)

The electronic properties of pristine and doped aluminene were analyzed based on calculations of the band structure and density of states (DOS), explicitly taking into account spin polarization (nspin=2). The corresponding figures (Fig. 6(a-b) , 7(a-h) and 8(a-j)) show a representative illustration of pristine aluminene and the doping effects for each system studied, with one image per material to avoid clutter.

3.4.1. Pristine Planar Aluminene

Pristine aluminene retains its metallic character, with bands crossing the Fermi level (E_F = 0 eV, Fig. 6.a). The pDOS (Fig. 6.b) reveals a strong contribution from aluminum's *p*-orbitals near the Fermi level, confirming its metallic behavior. These results are consistent with previous theoretical studies [5–7].

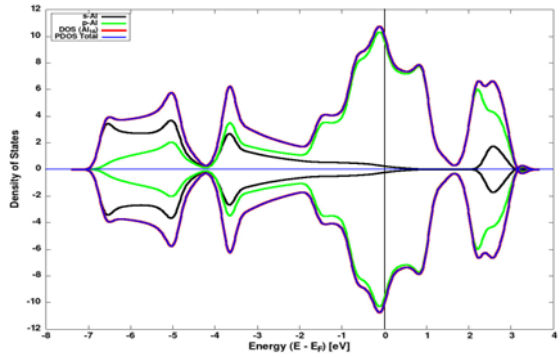

Figure 6a : **pDOS of pristine aluminene.**

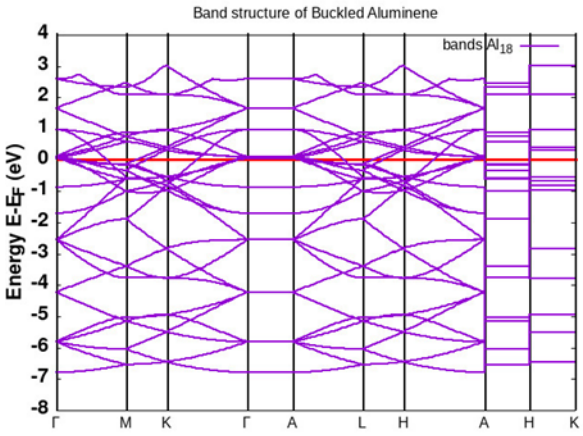

Figure 6b : **Bands structure of aluminene**

3.4.2. Doping with 3d Transition Metals

The introduction of 3*d* transition metals results in a marked modification of the electronic properties of aluminene (Fig. 7).

For dopants such as *Sc, Ti, Cu, and Zn*, the band structure retains its metallic character, with no notable spin polarization. This is consistent with the absence of magnetic moments for these systems, as discussed previously.

In contrast, for *V, Cr, Mn, and Fe* doped planar aluminene, a clear spin polarization of the electronic bands is observed, with a distinct separation between the spin-up (↑) and spin-down (↓) channels. The density of states (DOS) highlights the emergence of highly localized *d*-orbital states near the Fermi level E_F , which are directly responsible for the significant magnetic moments found in these systems (up to 5.38 $\mu_B/cell$ for Mn). This behavior confirms the potential of these specific dopants to induce magnetic properties in aluminene for spintronic applications.

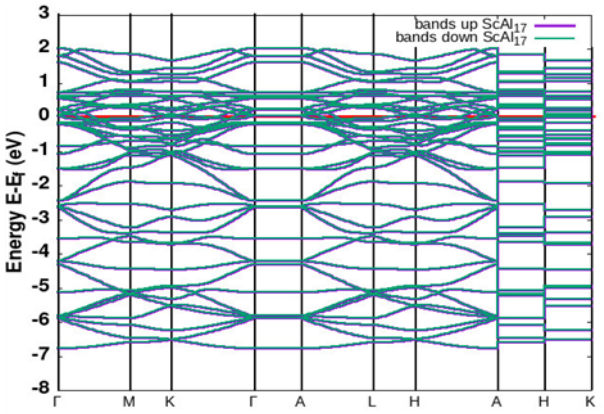

(a) Bands structure spin $ScAl_{17}$ (zoom near E_F)

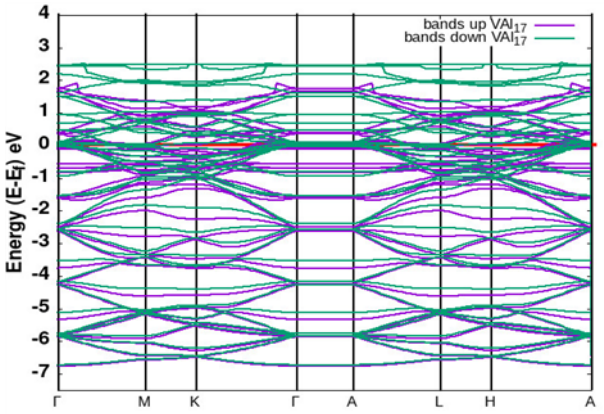

(b) Bands spin structure VAl_{17} (zoom near E_F)

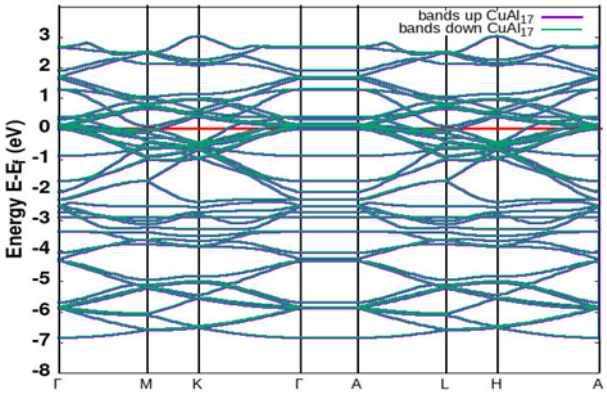

(c) Bands spin structure $CuAl_{17}$ (zoom near E_F)

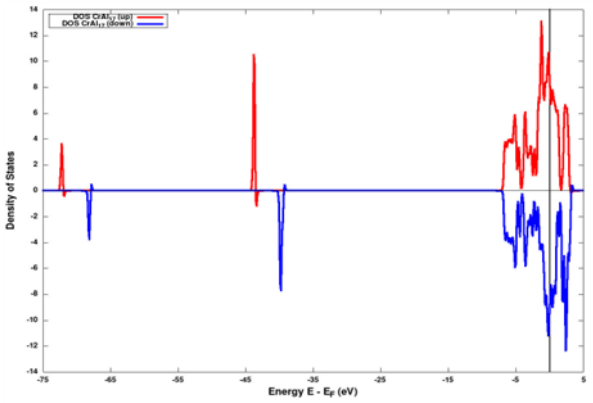

(d) DOS $CrAl_{17}$

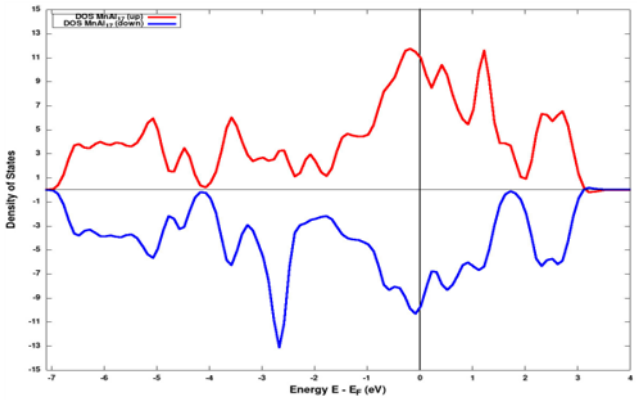

(e) DOS $MnAl_{17}$ (zoom near E_F)

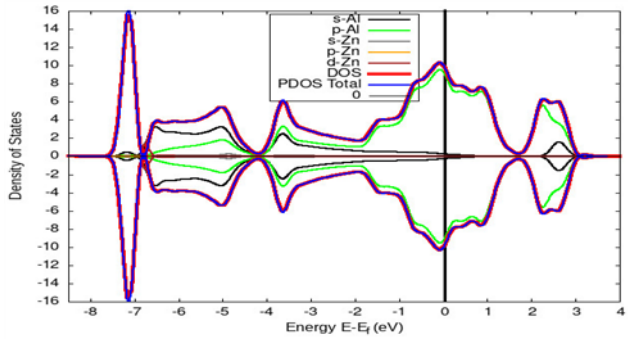

(f) pDOS $ZnAl_{17}$ (zoom near E_F)

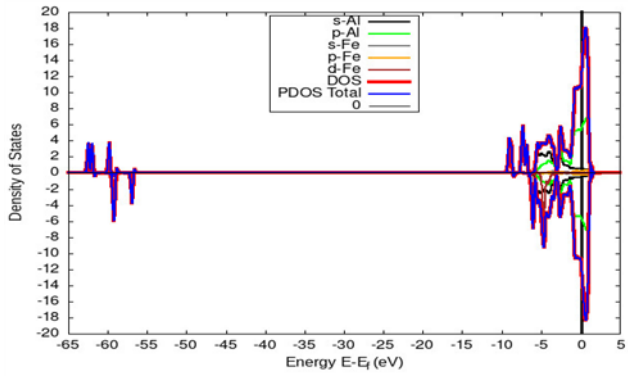

(g) pDOS $FeAl_{17}$

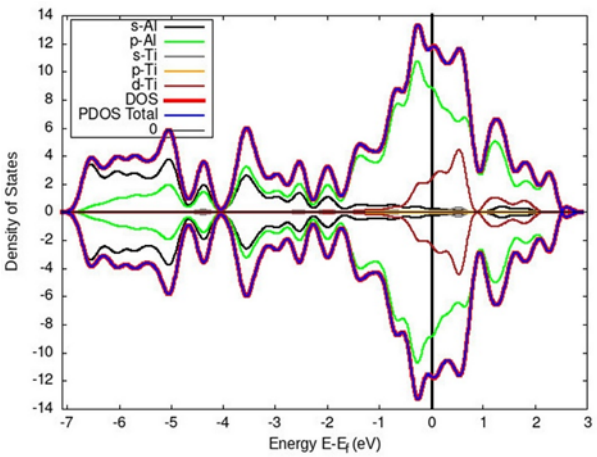

(h) pDOS $TiAl_{17}$ (zoom near E_F)

Figure 7 (a – h) : **Al-3d electronic properties**

3.4.3. Doping with 4d Transition Metals

The 4*d* series (figure 8) shows a similar trend but with generally more moderate effects.

Dopant like Y, Ag, and Cd retain an almost non-polarized metallic behavior, with no detectable magnetism.

TMs like Zr, Mo, Tc, Ru, and Nd induce a partial spin polarization of the DOS, with the appearance of localized *d*-states in the vicinity of the Fermi level. The hybridization between the dopant's *d*-orbitals and aluminum's *p*-orbitals leads to a net magnetization, although generally weaker than that observed with 3*d* dopants.

On other hands, Rh and Pd stand out due to an electronic symmetry breaking linked to the structural distortion ($\gamma \neq 120°$). This deformation results in a modification of the electronic dispersions and a notable lowering of the binding energy, but without associated magnetization.

This differentiated behavior clearly illustrates the key role of the dopant's electronic configuration and atomic size in the stabilization of electronic and magnetic states in doped aluminene.

As shown in Figure 8: *Al-4d electronic properties*, the electronic properties of 4*d*-doped aluminene are represented

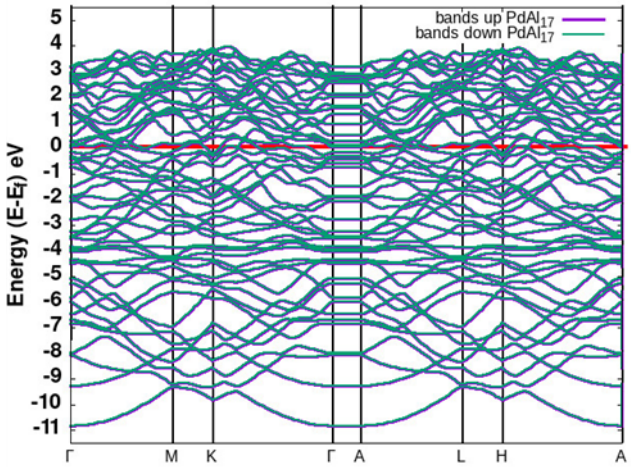

(a) Bands spin structure $PdAl_{17}$ (zoom near E_F)

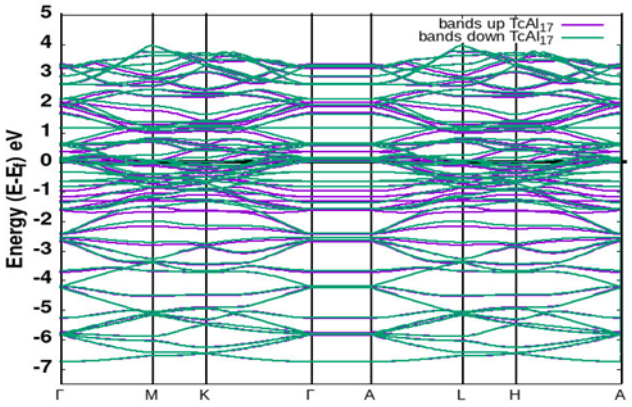

(b) Bands spin structure $TcAl_{17}$ (zoom near E_F)

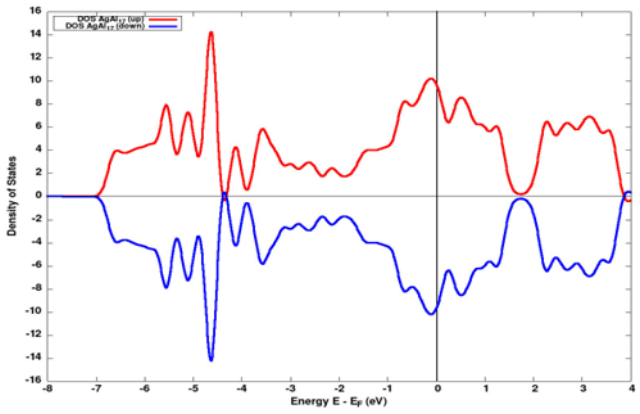

(c) DOS $AgAl_{17}$ (zoom near E_F)

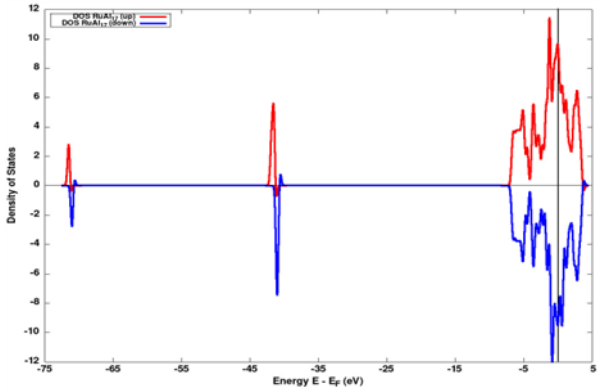

(d) DOS $RuAl_{17}$

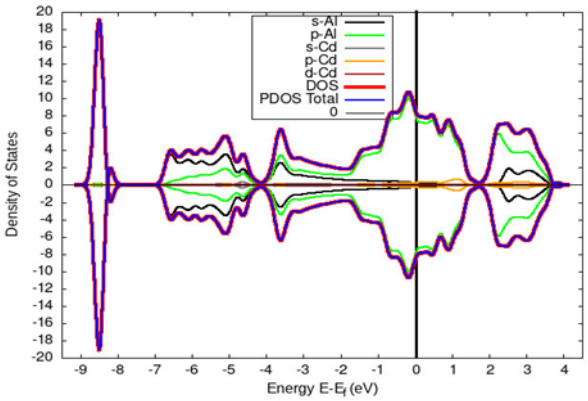

(e) PDOS $CdAl_{17}$

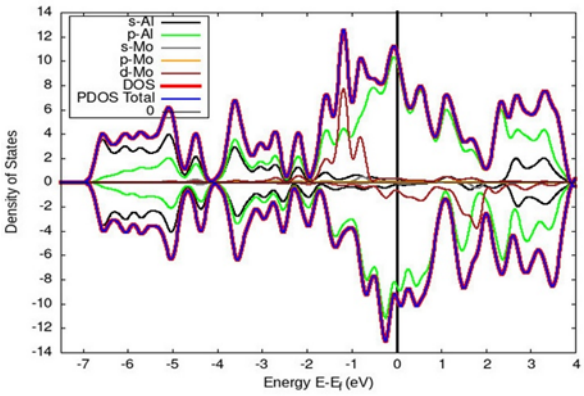

(f) pDOS $MoAl_{17}$ (zoom near E_F)

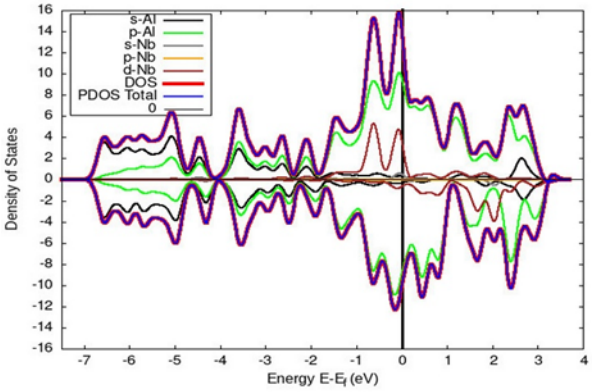

(g) pDOS $NbAl_{17}$ (zoom near E_F)

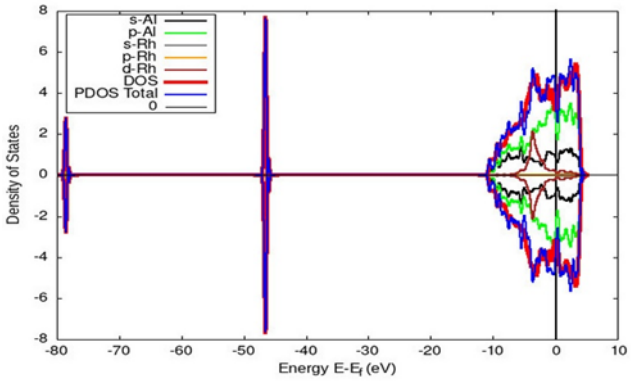

(h) pDOS $RhAl_{17}$

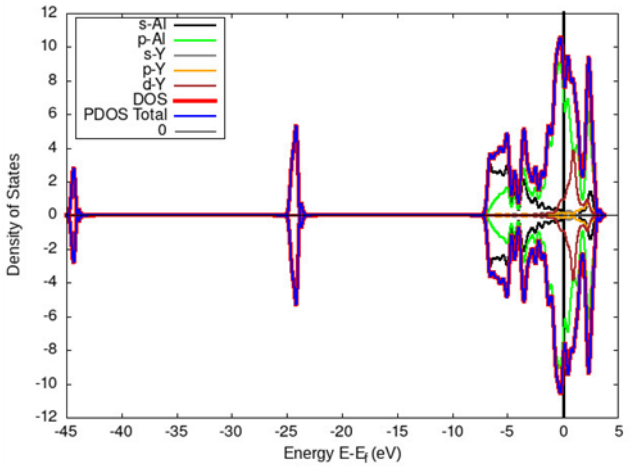

(i) pDOS YAl_{17}

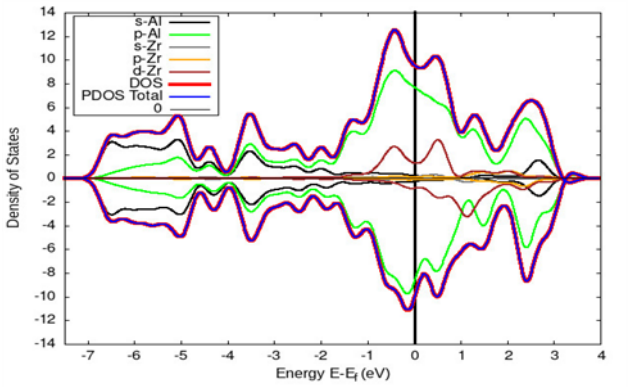

(j) PDOS $ZrAl_{17}$ (zoom near E_F)

Figure 8 (a – j) : **Al-4d electronic properties**

3.5. General Discussion

The results obtained in this study highlight the strong tunability of planar aluminene through substitutional doping with 3d and 4d transition metals. From a structural perspective, most doped systems preserve the hexagonal symmetry of pristine aluminene, with the notable exception of Rh- and Pd-doped configurations, where significant distortions are observed. These symmetry breakings are consistent with the larger atomic radii and specific bonding characteristics of late transition metals, which tend to destabilize the ideal honeycomb arrangement. Such structural distortions are not merely geometrical features but have direct consequences on the electronic dispersion and energetic stability of the system.

In terms of energetic stability, the calculated binding energies confirm that substitution with early transition metals (e.g., Sc, Ti, Y, Zr) and some late elements (Cu, Ag, Zn, Cd) results in relatively stable configurations, with binding energies close to or slightly lower than that of pristine aluminene. However, magnetic dopants such as Mn and Fe in the 3d series, and Mo, Tc, and Ru in the 4d series, show reduced energetic stability. This trade-off between stability and functionality is often reported in doped 2D systems, where the most magnetically active dopants are not always the most stable energetically.

From the electronicc perspective viewpoint, pristine aluminene remains metallic with dominant Al-p orbital contributions at the Fermi level. Doping with non-magnetic elements such as Sc, Ti, Cu, Zn, Y, Ag, and Cd essentially preserves this metallic nature without inducing spin polarization. In contrast, magnetic dopants such as V, Cr, Mn, Fe (3d), and Mo, Tc, Ru, Nd (4d) introduce localized d-states near the Fermi level, giving rise to strong p–d hybridization. This leads to significant spin polarization, as evidenced by the density of states (DOS) and band structures. These findings mirror trends reported in doped graphene and transition-metal dichalcogenides (TMDs). In graphene, for instance, incorporation of TMs like V, Cr, Mn, and Co induces stable magnetism through strong d–p hybridization, with spin polarization and density of states near the Fermi level directly linked to this interaction [13,4243,4344]. Similarly, in TMDs, dopants such as Mo and Nb modify electronic dispersion while activating sizable magnetic moments [10,4445]. These parallels confirm that hybridization between the dopant's d orbitals and the host lattice's p orbitals is the key mechanism governing magnetism in aluminene as in other 2D systems.

A particularly striking outcome is the emergence of large magnetic moments, especially for Mn (≈5.38 μ_B⁄cellμB/cell) and Cr, positioning these doped systems as strong candidates for spintronic applications. The robustness of these induced moments, combined with metallic conductivity, suggests potential integration into spin-polarized transport devices. Nonetheless, the balance between structural stability and magnetic enhancement remains a critical challenge, as highly magnetic dopants often introduce larger lattice distortions. For elements like Rh and Pd, our results show symmetry breaking without magnetism, consistent with previous reports in graphene [11,4344], further illustrating the sensitivity of electronic properties to the choice of dopant.

Overall, the results demonstrate that planar aluminene constitutes a highly versatile 2D platform whose properties can be engineered through transition metal doping. The systematic trends observed between 3d and 4d dopants provide a roadmap for designing

aluminene-based devices with tailored magnetic and electronic functionalities, while also raising fundamental questions on the interplay between structural distortion, energetic stability, and induced magnetism in purely metallic 2D lattices.

4. Conclusion

This theoretical study, based on ab initio calculations, has provided a comprehensive investigation of the effects of 3d and 4d transition metal doping on the structural, energetic, and electronic properties of planar aluminene. Our results confirm that aluminene is a highly versatile two-dimensional platform whose properties can be finely tuned through substitutional doping.

Structurally, pristine aluminene preserves its hexagonal symmetry, in excellent agreement with previous studies. Most dopants maintain this symmetry; however, significant distortions were observed in the Rh- and Pd-doped systems. These distortions are attributed to the specific hybridization of the dopants' d-orbitals, reflecting a fundamental trade-off between structural integrity and energetic stability.

Regarding electronic and magnetic properties, our study reveals promising perspectives for spintronic applications. While pristine aluminene is non-magnetic, the introduction of 3d dopants (V, Cr, Mn, Fe) and 4d dopants (Zr, Mo, Tc, Ru, Nd) induces substantial magnetic moments arising from the hybridization between the dopant d-orbitals and the host p-orbitals. Notably, manganese (Mn) induces a negative total magnetization, a unique effect that merits further investigation. Additionally, we observed that the most energetically stable doped systems are often non-magnetic, highlighting a key consideration for practical device design.

In summary, this study provides a detailed roadmap for engineering doped aluminene and designing tailored two-dimensional materials for spintronic and electronic devices. The systematic trends observed between 3d and 4d dopants establish a solid foundation for further investigations, particularly regarding the complex interplay between structural distortions, energetic stability, and magnetic behavior.

5. Perspectives

Although this study provides valuable insights into transition metal doping in planar aluminene, several research directions remain open. Future studies should explore the electronic transport properties, including spin-polarized conductivity and magnetoresistance effects, to better assess the material's potential for spintronic devices. The incorporation of spin-orbit coupling could reveal topological or anisotropic phenomena not captured in the present approach.

Moreover, the influence of Van der Waals interactions with realistic substrates should be investigated to evaluate experimental feasibility. Additional strategies, such as co-doping, defect engineering, or mechanical strain, could offer further routes to tailor aluminene's properties. Finally, experimental validation is essential to confirm these theoretical predictions and to enable the practical development of next-generation devices based on doped aluminene.

Acknowledgements

We thank the African School on Electronic Structure Methods and Applications (ASESMA 2023) for their teachings, which greatly enriched this work. We would also like to acknowledge the use of the facilities at the Centre for High Performance Computing (CHPC) in Cape Town, South Africa, which were essential for this work. We are also grateful to Professor Nithaya Chetty and Dr. Noeliarinala Felana Andriambelaza for their support and guidance.

REFERENCES

[1] Novoselov, K. S., Geim, A. K., Morozov, S. V., Jiang, D., Zhang, Y., Dubonos, S. V., Grigorieva, I. V., Firsov, A. A. Electric Field Effect in Atomically Thin Carbon Films. Science, 306(5696), 666–669 (2004). DOI: 10.1126/science.1102896

[2] Vogt, P., De Padova, P., Quaresima, C., Avila, J., Frantzeskakis, E., Asensio, M. C., Resta, A., Ealet, B., Le Lay, G. Silicene: Compelling Experimental Evidence for Graphenelike Two-Dimensional Silicon. Physical Review Letters, 108(15), 155501 (2012). DOI: 10.1103/PhysRevLett.108.155501

[3] Liu, H., Neal, A. T., Zhu, Z., Luo, Z., Xu, X., Tománek, D., Ye, P. D. Phosphorene: An Unexplored 2D Semiconductor with a High Hole Mobility. ACS Nano, 8(4), 4033–4041 (2014). DOI: 10.1021/nn501226z

[4] Chhowalla, M., Shin, H. S., Eda, G., Li, L.-J., Loh, K. P., Zhang, H. The Chemistry of Two-Dimensional Layered Transition Metal Dichalcogenide Nanosheets. Nature Chemistry, 5(4), 263–275 (2013). DOI: 10.1038/nchem.1589

[5] Kamal, C., Chakrabarti, A., Ezawa, M. Aluminene as Highly Hole-Doped Graphene. New Journal of Physics, 17(8), 083014 (2015). DOI: 10.1088/1367-2630/17/8/083014

[6] Yuan, J., Yu, N., Xue, K., Miao, X. Stability, Electronic and Thermodynamic Properties of Aluminene from First-Principles Calculations. Applied Surface Science, 409, 85–90 (2017). DOI: 10.1016/j.apsusc.2017.02.238

[7] Sene, P., Dioum, A., Ndiaye, S., Gueye, E. H. O., Talla, K., Beye, A. C. Stability, Electronic and Structural Properties of Aluminene from First-Principles Calculations. MRS Advances, 8(14), 666–680 (2023). https://doi.org/10.1557/s43580-023-00625-y

[8] Malek, A., Movlarooy, T., & Pilehrood, S. (2022). Transition metals doped (3,3) armchair boron nitride nanosheet as dilute magnetic semiconductors materials for the spintronic application. International Journal of Quantum Chemistry. https://doi.org/10.1002/qua.27070

[9] Krasheninnikov, A. V., Lehtinen, P. O., Foster, A. S., Pyykkö, P., Nieminen, R. M. Embedding Transition-Metal Atoms in Graphene: Structure, Bonding, and Magnetism. Physical Review Letters, 102(12), 126807 (2009). DOI: 10.1103/PhysRevLett.102.126807

[10] Abdelati, M. A., Maarouf, A. A., Fadlallah, M. M. Substitutional Transition Metal Doping in $MoSi_2N_4$ Monolayer: Structural, Electronic and Magnetic Properties. Physical Chemistry Chemical Physics, 24(6), 3035–3045 (2022). DOI: 10.1039/D1CP04191F

[11] Yoo, H., Heo, K., Ansari, M. H. R., Cho, S. Recent Advances in Electrical Doping of 2D Semiconductor Materials: Methods, Analyses, and Applications. Nanomaterials, 11(4), 832 (2021). DOI: 10.3390/nano11040832
[12] Chen, W., Chen, Q., Zhang, J., Zhou, L., Tang, W., Wang, Z., Deng, J., Wang, S. Electronic and Magnetic Properties of Transition-Metal-Doped Monolayer B_2S_2 within GGA+U Framework. RSC Advances, 14(9), 3390–3399 (2024). DOI: 10.1039/D3RA08472H
[13] Hernández-Tecorralco, J., Meza-Montes, L., Cifuentes-Quintal, M. E., de Coss, R. Understanding the sp Magnetism in Substitutional Doped Graphene. Physical Review B, 105(22), 224425 (2022). DOI: 10.1103/PhysRevB.105.224425
[14] Nair, R. R., Sepioni, M., Tsai, I. L., Lehtinen, O., Keinonen, J., Krasheninnikov, A. V., Thomson, T., Geim, A. K., Grigorieva, I. V. Spin-Half Paramagnetism in Graphene Induced by Point Defects. Nature Physics, 8(3), 199–202 (2012). DOI: 10.1038/nphys2183
[15] Giannozzi, P., Baroni, S., Bonini, N., Calandra, M., Car, R., Cavazzoni, C., Ceresoli, D., Chiarotti, G. L., Cococcioni, M., Dabo, I., et al. QUANTUM ESPRESSO: A Modular and Open-Source Software Project for Quantum Simulations of Materials. Journal of Physics: Condensed Matter, 21(39), 395502 (2009). DOI: 10.1088/0953-8984/21/39/395502
[16] Giannozzi, P., Andreussi, O., Brumme, T., Bunau, O., Nardelli, M. B., Calandra, M., Car, R., Cavazzoni, C., Ceresoli, D., Cococcioni, M., et al. Advanced Capabilities for Materials Modelling with Quantum ESPRESSO. Journal of Physics: Condensed Matter, 29(46), 465901 (2017). DOI: 10.1088/1361-648X/aa8f79
[17] Zhu, H., Gan, X., McCreary, A., Lv, R., Lin, Z., Terrones, M. Heteroatom Doping of Two-Dimensional Materials: From Graphene to Chalcogenides. Nano Today, 30, 100829 (2020). DOI: 10.1016/j.nantod.2019.100829
[18] Liu, J., Li, Q. Two-Dimensional Doped Materials. Magnetochemistry, 8(12), 172 (2022). DOI: 10.3390/magnetochemistry8120172
[19] Wang, D., Li, X., Sun, H. Modulation Doping: A Strategy for 2D Materials Electronics. Nano Letters, 21(21), 9037–9045 (2021). DOI: 10.1021/acs.nanolett.1c02192
[20] Loh, L., Zhang, Z., Bosman, M., Eda, G. Substitutional Doping in 2D Transition Metal Dichalcogenides. Nano Research, 14(6), 1668–1681 (2020). DOI: 10.1007/s12274-020-3013-4
[21] Wang, Z., Xia, H., Wang, P., Zhou, X., Liu, C., Zhang, Q., Wang, F., Huang, M., Chen, S., Wu, P., Chen, Y., Ye, J., Huang, S., Yan, H., Gu, L., Miao, J., Li, T., Chen, X., Lu, W., Zhou, P., Hu, W. Controllable Doping in 2D Layered Materials. Advanced Materials, 33(47), 2104942 (2021). DOI: 10.1002/adma.202104942
[22] Kumar, R., Sahoo, S., Joanni, E., Singh, R., Tan, W., Moshkalev, S., Matsuda, A., Kar, K. Heteroatom Doping of 2D Graphene Materials for Electromagnetic Interference Shielding: A Review of Recent Progress. Critical Reviews in Solid State and Materials Sciences, 47(6), 570–619 (2021). DOI: 10.1080/10408436.2021.1965954
[23] Kumar, R., Shringi, A., Wood, H., Asuo, I., Oturak, S., Sanchez, D., Sharma, T., Chaurasiya, R., Mishra, A., Choi, W., Doumon, N., Dabo, I., Terrones, M., Yan, F. Substitutional Doping of 2D Transition Metal Dichalcogenides for Device Applications: Current Status, Challenges and Prospects. Materials Science and Engineering: R: Reports, 180, 100946 (2025). DOI: 10.1016/j.mser.2025.100946
[24] Zhang, X., Gao, L., Yu, H., Liao, Q., Kang, Z., Zhang, Z., Zhang, Y. Single-Atom Vacancy Doping in Two-Dimensional Transition Metal Dichalcogenides. Accounts of Materials Research, 2(11), 1017–1025 (2021). DOI: 10.1021/ACCOUNTSMR.1C00097
[25] Pandey, D., Kamal, C., Chakrabarti, A. First-Principles Study of Adsorption of 3d and 4d Transition Metal Atoms on Aluminene. Computational Condensed Matter, 17, e00319 (2018). DOI: 10.1016/j.cocom.2018.e00319
[26] Pedrosa, G. R., Villagracia, A. R., Bayasen, D. S., Lin, H., Ong, H., David, M., & Arboleda, N. B. First Principles Investigation on the Nitrogen-Doped Planar Aluminene for Hydrogen Storage Application. IOP Conference Series: Earth and Environmental Science, 463, 012103 (2020). https://doi.org/10.1088/1755-1315/463/1/012103
[27] Pandey, D., Kamal, C., & Chakrabarti, A. (2019). Strain induced magnetism and half-metallicity in alkali metal substituted aluminene. DAE SOLID STATE PHYSICS SYMPOSIUM 2018. https://doi.org/10.1063/1.5113190
[28] Pandey, D., Kumar, S., Kumar, A., & Pathak, B. Improved Gas Adsorption on Functionalized Aluminene Surface: A First-Principles Study. Applied Surface Science, 531, 147364 (2020). https://doi.org/10.1016/j.apsusc.2020.147364
[29] Villagracia, A., Sugimoto, K., Raghunathan, A., Goddard, W. A., III. First Principles Investigation on the Elastic Properties of Mg, Ca, K-decorated Planar Aluminene. 2019 IEEE 11th International Conference on Humanoid, Nanotechnology, Information Technology, Communication and Control, Environment, and Management (HNICEM) (pp. 1–5). IEEE (2019). DOI: 10.1109/HNICEM48295.2019.9073435
[30] Villagracia, A., Sugimoto, K., Goddard, W. A., III. First Principles Investigation on the Hydrogen Adsorption on Planar Aluminene with Boron, Carbon, and Nitrogen as Impurities. Molecular Physics, 120(6), e2086182 (2022). DOI: 10.1080/00268976.2022.2086182
[31] Perdew, J. P., Ruzsinszky, A., Csonka, G. I., Vydrov, O. A., Scuseria, G. E., Constantin, L. A., Zhou, X., & Burke, K. (2008). Restoring the Density-Gradient Expansion for Exchange in Solids and Surfaces. Physical Review Letters, 100,136406. https://doi.org/10.1103/PhysRevLett.100.136406
[32] Blöchl, P. E. (1994). Projector augmented-wave method. Phys. Rev. B, 50, 17953. DOI: 10.1103/PhysRevB.50.17953
[33] Vanderbilt, D. (1990). Soft self-consistent pseudopotentials in a generalized eigenvalue formalism. Phys. Rev. B, 41, 7892. https://doi.org/10.1103/PhysRevB.41.7892
[34] D. R. Hamann, "Optimized norm-conserving Vanderbilt pseudopotentials," Phys. Rev. B 88, 085117 (2013)
[35] G. Prandini, A. Marrazzo, I. E. Castelli, N. Mounet, and N. Marzari (2018). Standard Solid-State Pseudopotentials (SSSP) library... npj Comput. Mater., 4, 72. DOI: 10.1038/s41524-018-0100-3
[36] Materials Cloud, QE Input Generator. Consulté à l'adresse : https://qeinputgenerator.materialscloud.io/compute/process_structure/. Last access September 18, 2025
[37] Dal Corso, A. (2014). Pseudopotentials periodic table: From H to Pu. Comput. Mater. Sci., 95, 337–350. DOI: 10.1016/j.commatsci.2014.07.043
[38] K. F. Garrity, J. W. Bennett, K. M. Rabe, and D. Vanderbilt, (2014). Pseudopotentials for high-throughput DFT calculations. Comput. Mater. Sci., 81, 446–452. DOI: 10.1016/j.commatsci.2013.09.005
[39] A. Togo, I. Tanaka, Scripta Mater. 108, 1–5 (2015).
[40] Du, L., Hasan, T., Castellanos-Gómez, A., Liu, G., Yao, Y., Lau, C., & Sun, Z. (2021). Engineering symmetry breaking in 2D layered materials. Nature Reviews Physics, 3, 193 - 206. https://doi.org/10.1038/s42254-020-00276-0
[41] Zhang, M., Han, N., Wang, J., Zhang, Z., Liu, K., Sun, Z., Zhao, J., & Gan, X. (2022). Strong Second Harmonic

Generation from Bilayer Graphene with Symmetry Breaking by Redox-Governed Charge Doping.. Nano letters. https://doi.org/10.1021/acs.nanolett.1c04359
[42] Zhang, Y., Huang, D., Shan, Y., Jiang, T., Zhang, Z., Liu, K., Shi, L., Cheng, J., Sipe, J., Liu, W., & Wu, S. (2018). Doping-Induced Second-Harmonic Generation in Centrosymmetric Graphene from Quadrupole Response.. Physical review letters, 122 4, 047401. https://doi.org/10.1103/PhysRevLett.122.047401
[43] Paidi, V., Jung, E., Lee, J., Lee, A., Shepit, M., Ihm, K., Lee, B., Van Lierop, J., Hyeon, T., & Lee, K. (2022). Robust Room Temperature Ferromagnetism In Cobalt Doped Graphene by Precision Control of Metal Ion Hybridization. Advanced Functional Materials, 33. https://doi.org/10.1002/adfm.202210722
[44] Tuček, J., Błoński, P., Ugolotti, J., Swain, A., Enoki, T., & Zbořil, R. (2018). Emerging chemical strategies for imprinting magnetism in graphene and related 2D materials for spintronic and biomedical applications.. Chemical Society reviews, 47 11, 3899-3990. https://doi.org/10.1039/c7cs00288b
[45] Nguyen, D., Guerrero-Sanchez, J., & Hoat, D. (2024). Searching for new two-dimensional spintronic materials: Doping-induced magnetism in graphene-like SrS monolayer. Physica E: Low-dimensional Systems and Nanostructures. https://doi.org/10.1016/j.physe.2024.116003